



# A Summary of the Mechanical Properties Data Developed in FY 2023 by ANL, INL, and ORNL to Support the Data Package Development for the A709 Code Case

September 2023

Heramb Mahajan, Ting-Leung Sham  
*Idaho National Laboratory*

Yanli Wang, Zhili Feng  
*Oak Ridge National Laboratory*

Xuan Zhang  
*Argonne National Laboratory*



*INL is a U.S. Department of Energy National Laboratory  
operated by Battelle Energy Alliance, LLC*

#### **DISCLAIMER**

This information was prepared as an account of work sponsored by an agency of the U.S. Government. Neither the U.S. Government nor any agency thereof, nor any of their employees, makes any warranty, expressed or implied, or assumes any legal liability or responsibility for the accuracy, completeness, or usefulness, of any information, apparatus, product, or process disclosed, or represents that its use would not infringe privately owned rights. References herein to any specific commercial product, process, or service by trade name, trade mark, manufacturer, or otherwise, does not necessarily constitute or imply its endorsement, recommendation, or favoring by the U.S. Government or any agency thereof. The views and opinions of authors expressed herein do not necessarily state or reflect those of the U.S. Government or any agency thereof.

**A Summary of the Mechanical Properties Data  
Developed in FY 2023 by ANL, INL, and ORNL to  
Support the Data Package Development for the A709  
Code Case**

**Heramb Mahajan, Ting-Leung Sham  
Idaho National Laboratory  
Yanli Wang, Zhili Feng  
Oak Ridge National Laboratory  
Xuan Zhang  
Argonne National Laboratory**

**September 2023**

**Idaho National Laboratory  
Advanced Reactor Technologies  
Idaho Falls, Idaho 83415**

**<http://www.art.inl.gov>**

**Prepared for the  
U.S. Department of Energy  
Office of Nuclear Energy  
Under DOE Idaho Operations Office  
Contract DE-AC07-05ID14517**

*Page intentionally left blank*

## INL ART Program

# A Summary of the Mechanical Properties Data Developed in FY 2023 by ANL, INL, and ORNL to Support the Data Package Development for the A709 Code Case

INL/RPT-23-74680

September 2023

### Technical Reviewer:



---

Tate Patterson  
Welding Engineer

09/19/2023

---

Date

### Approved by:



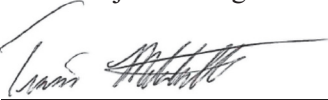
---

Michael E. Davenport  
ART Project Manager

9/19/2023

---

Date



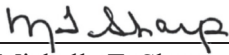
---

Travis R. Mitchell  
ART Program Manager

9/19/2023

---

Date



---

Michelle T. Sharp  
INL Quality Assurance

9/19/2023

---

Date

*Page intentionally left blank*

## **SUMMARY**

This report provides the status of tensile, creep, fatigue, and creep-fatigue testing to date conducted at Argonne National Laboratory, Idaho National Laboratory, and Oak Ridge National Laboratory to generate the data package required to qualify Alloy 709 in American Society of Mechanical Engineers, Boiler and Pressure Vessel Code, Section III, Division 5. The Division 5 Class A Alloy 709 Code Case requires data generated from a minimum of three commercial heats. Extensive mechanical properties data have been generated on two commercial heats, and some initial test data have been generated from the third commercial heat. The room temperature tensile test results for the three commercial heats met the specification minimum of the American Society of Mechanical Engineers, Boiler and Pressure Vessel Code, Section II, Part A, SA-213/SA-213M for Grade TP310MoCbN (UNS S31025) seamless tubing. These three commercial heats of Alloy 709 are suitable for generating the code case data.

*Page intentionally left blank*



## **ACKNOWLEDGEMENTS**

This research was sponsored by the US Department of Energy (DOE) under Contract No. DE-AC07-05ID14517 with Idaho National Laboratory (INL), which is managed and operated by Battelle Energy Alliance, LLC; under Contract No. DE-AC05-00OR22725 with Oak Ridge National Laboratory (ORNL), which is managed and operated by UT-Battelle, LLC; and under Contract No. DE-AC02-06CH11357 with Argonne National Laboratory (ANL), which is managed and operated by the University of Chicago–Argonne, LLC.

Programmatic direction was provided by the Office of Nuclear Reactor Deployment of the DOE Office of Nuclear Energy (NE). The authors gratefully acknowledge the support provided by Sue Lesica of DOE-NE, Federal Materials Lead for the Advanced Reactor Technologies (ART) Program; Kaatrin Abbott of DOE-NE, Federal Manager, ART Fast Reactor Program (FRP); and Bo Feng of ANL, National Technical Director, ART FRP.

The authors also acknowledge support from Richard Wright of Structural Alloys, LLC and thank Wesley Jones and Joel Simpson of INL for their testing support.

*Page intentionally left blank*

## CONTENTS

SUMMARY .....	vii
ACKNOWLEDGEMENTS .....	ix
ACRONYMS .....	xiii
1. INTRODUCTION .....	1
2. MATERIAL .....	2
3. TENSILE CODE CASE TESTING .....	3
4. CREEP CODE CASE TESTING .....	5
5. FATIGUE AND CREEP-FATIGUE CODE CASE TESTING .....	7
6. WELDS AND WELDMENT DEVELOPMENT .....	13
6.1 Fabrication and Qualification Testing of A709 Production Welds .....	13
6.2 Code Case Testing of A709 Welds .....	15
7. SUMMARY .....	15
8. REFERENCE .....	15

## FIGURES

Figure 1. A709 tensile code case testing specimen geometry. All dimensions are in inches. ....	3
Figure 2. (a) Yield strength, (b) ultimate tensile strength, (c) % elongation, and (d) % reduction of area against temperature of A709-PT materials. ....	5
Figure 3. Creep code case testing in support of the staged code qualification plan.....	6
Figure 4. Finished and ongoing creep tests to support code case development on three commercial heats. ....	6
Figure 5. Creep-rupture data collected to date for the applied stresses and test temperatures shown. A709-PT materials from the three commercial heats.....	7
Figure 6. Test specimen geometry used at INL for fatigue and creep-fatigue tests. All dimensions are in inches. ....	8
Figure 7. Test specimen geometry used at ORNL for fatigue and creep-fatigue tests. All dimensions are in inches. ....	9
Figure 8. Schematic of the failure criterion to determine the cycles to failure in fatigue and creep-fatigue tests. ....	10
Figure 9. Number of cycles to failure against the applied strain range from the fatigue tests for the A709-PT materials from the first and second commercial heat for different temperatures.....	10
Figure 10. Comparison of the peak-and-valley stress plots for fatigue tests at 954°C with different strain ranges. ....	11
Figure 11. Schematic figure showing a typical strain-controlled creep-fatigue load cycle. ....	11

Figure 12. Creep-fatigue data plotted in the form of a creep-fatigue interaction diagram for A709-PT materials from three commercial heats. ....	12
Figure 13. Photographs of the A709 production welds: (a) W10 and (b) W11. ....	14

## TABLES

Table 1. Information on the three A709 commercial heats for code case testing. ....	2
Table 2. Chemical composition of three commercial heats of A709 (wt. %). ....	2
Table 3. RT tensile properties of A709-PT from the three commercial heats. ....	4
Table 4. Summary of the creep code case testing on A709-PT from the three commercial heats. ....	6
Table 5. A709 production welds. ....	13

## ACRONYMS

ANL	Argonne National Laboratory
AOD	Argon-oxygen decarburization
ART	Advanced Reactor Technologies
ASME	American Society of Mechanical Engineers
ASTM	American Society for Testing and Materials
BPVC	Boiler and Pressure Vessel Code
CC	Code Case
DOE	Department of Energy
ESR	Electroslag remelting
FY	Fiscal Year
GTAW	Gas tungsten arc welding
INL	Idaho National Laboratory
NE	Nuclear Energy
ORNL	Oak Ridge National Laboratory
PT	Precipitation treatment
RT	Room temperature
SA	Solution Annealing
SFR	Sodium-cooled Fast Reactors
UNS	Unified Numbering System
UTS	Ultimate tensile strength
wppm	weight parts per million
YS	Yield Strength

*Page intentionally left blank*

# **A Summary of the Mechanical Properties Data Developed in FY 2023 by ANL, INL, and ORNL to Support the Data Package Development for the A709 Code Case**

## **1. INTRODUCTION**

Early deployment of advanced reactor systems is an overarching driver for nuclear energy to contribute to the race to zero carbon emission. Sodium-cooled fast reactor (SFR) is a mature advanced reactor technology. But to support early deployment of SFRs, the construction costs must come down. The objective of the advanced materials development activity of the Fast Reactors Campaign of the Advanced Reactor Technologies (ART) Program within the Office of Nuclear Energy (NE) of the Department of Energy (DOE) is to develop and qualify advanced structural materials to enable improved reactor performance. Improved structural material performance can reduce costs of fast reactors by potentially allowing both higher operating temperatures (and thus, higher thermal efficiency and power output) and longer lifetimes for components. Improved materials reliability could also result in reduced downtime. Superior structural materials will also spur improvements in high-temperature design methodology, and thereby allow more flexibility in construction and operation. Advancements in material performance enable greater safety margins and more stable performance over a longer lifetime.

A multi-laboratory effort involving Argonne National Laboratory (ANL), Idaho National Laboratory (INL), and Oak Ridge National Laboratory (ORNL) was initiated to conduct alloy optimization and properties evaluation. Based on its overall superior mechanical performance over 316H stainless steel, a reference construction material for SFR, A709 was recommended by the three-laboratory team for qualification in the American Society of Mechanical Engineers (ASME) Boiler and Pressure Vessel Code (BPVC) Section III, Division 5 [1], which provides the construction rules for advanced reactor components operating in the creep regime under cyclic service. Development of a Section III, Division 5 material code case for Class A construction requires design data from a minimum of three commercial heats. A staged code qualification plan for A709 was developed by the three-laboratory team and a description of the test plan can be found in Sham and Natesan's 2017 conference paper [2].

Currently, the Fast Reactors Campaign of the ART Program is developing A709 data package to support the development of Section III, Division 5 code cases per the staged code qualification plan. Significant work has been done to understand and develop material properties for the A709 code cases [3-5]. These studies have explored the influence of different heat treatments on microstructure and elevated temperature mechanical properties [3, 5]. The solution annealing (SA) temperature of 1150°C, or higher, yielded best creep properties but with less than optimum creep-fatigue properties. An additional precipitation treatment (PT) of 775°C for 10 hours resulted in the precipitation of beneficial Nb-rich nano precipitates that are likely the MX (Nb(C, N)) and Z-phase (CrNbN). These precipitate formations delay nitride and carbo-nitride formation, which improved creep-fatigue properties and achieved a balanced creep and creep-fatigue properties for the A709 materials in the PT condition.

The objective of this report is to provide an update on the progress in the code case testing program on the precipitation treated A709 material, to be referred to as A709-PT, at ANL, INL and ORNL. The mechanical properties testing includes tensile, creep, fatigue, and creep-fatigue in the air environment. Extensive test data from two commercial heats and initial test results from the third commercial heat are presented in this report.

## 2. MATERIAL

The DOE-NE ART Program procured the following three commercial heats of A709 in plate product form. The first commercial heat was fabricated by G.O. Carlson. The second and third heats were fabricated by ATI Specialty Rolled Products. All plate materials used for the code case testing were produced by argon-oxygen-decarburization (AOD) followed by electroslag remelting (ESR) to produce the ingots. The ingots were then hot rolled into the plate product form. The as-rolled plates were given a solution anneal treatment at a minimum temperature of 1150°C hours. All materials are given a heat treatment of 775°C for 10 hours in air followed by air cooling. This heat treatment is referred as precipitation treatment (PT). Mechanical properties testing is performed on the PT materials in support of the development of A709 code cases. Table 1 summarizes the detailed information of the three commercial heats procured, listing the weights, nominal grain size, and plate thicknesses. It also lists the plate IDs from the three commercial heats where test specimens are fabricated to support the A709 code case testing.

Table 1. Information on the three A709 commercial heats for code case testing.

	Material Details			Plate IDs used for Code Case Testing	Nominal ASTM Grain Size Number	Nominal Plate Thickness (in.)
	Fabricator	Master Heat Number	Procured Amount (lbs)			
Heat 1	G.O. Carlson Inc	58776	45,000	58776-3RBC1	7	1.10
Heat 2	ATI Specialty Rolled Products	529900	41,000	CG05455, CG05368	7	1.75
Heat 3		530843	38,000	CG45192	4	1.75

Note: Minimum solution annealing temperature of 1150°C for all procured heats.

All specimens were machined from plates along the rolling direction. The specimens used for the code case testing were machined from the mid-thickness location for commercial heat 1 and at the one-quarter thickness locations for commercial Heats 2 and 3. Table 2 documents the chemical compositions that were provided in the vendor material certification for all three heats. The chemistry specification for A709 in seamless tubing form as found in the ASME BPVC SA213/SA213M-23 specification [6] for Grade TP310MoCbN with a Unified Number System (UNS) designation of S31025 is also listed in Table 2 for reference.

Table 2. Chemical composition of three commercial heats of A709 (wt. %).

Element*	Commercial Heat 1	Commercial Heat 2	Commercial Heat 3	ASME SA-213 Specification for UNS S31025
	Heat Number 58776	Heat Number 529900	Heat Number 530843	
C	0.066	0.08	0.07	0.10 max
Cr	20.05	19.9	19.8	19.5–23.0
Co	0.02	0.02	0.01	—
Ni	25.14	24.6	25	23.0–26.0
Mn	0.9	0.9	0.9	1.50 max
Mo	1.51	1.5	1.5	1.0–2.0
N	0.152	0.15	0.15	0.10–0.25



Element*	Commercial Heat 1	Commercial Heat 2	Commercial Heat 3	ASME SA-213 Specification for UNS S31025
	Heat Number 58776	Heat Number 529900	Heat Number 530843	
Si	0.38	0.39	0.44	1.00 max
P	0.014	0.003	0.008	0.030 max
S	0.001	<0.001	0.001	0.030 max
Ti	0.01	<0.01	< 0.01	0.20 max
Nb	0.26	0.17	0.18	0.10–0.40
Al	0.02	0.02	0.02	—
B	0.003	0.004	0.005	0.002–0.010
Cu	0.06	0.06	0.04	—

\*The balance element is Fe.

### 3. TENSILE CODE CASE TESTING

An extensive set of tensile tests were conducted on A709-PT from the three commercial heats at a wide temperature range, from room temperature (RT) to 1000°C, at ORNL. The geometry of the tensile specimen is shown in Figure 1. All tensile test specimens were machined along the rolling direction of the A709 plates. The tensile test procedure followed ASTM E8/E8M-21 [7] at RT, and ASTM E21 [8] at elevated temperatures.

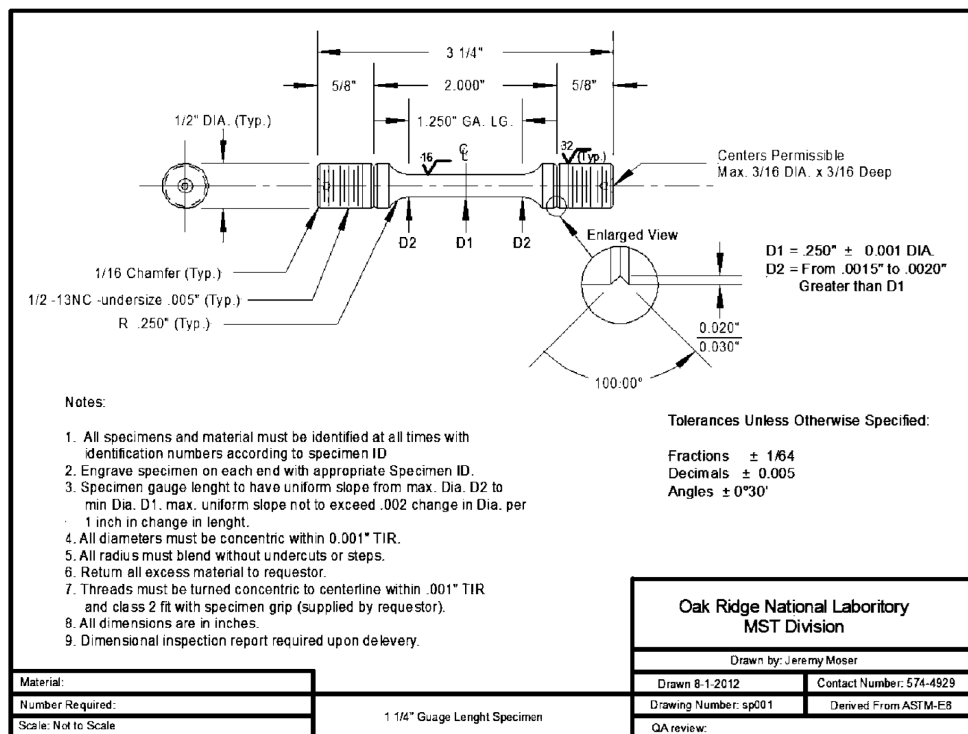


Figure 1. A709 tensile code case testing specimen geometry. All dimensions are in inches.

In Fiscal Year (FY) 2023, tensile code case testing on commercial Heat 3 (Heat 530843) was started. And the results are updated in Table 3 and Figure 2. The tensile code case testing matrix on all three heats is expected to be completed in FY 2024.

Table 3 compares the yield strength (YS) calculated with 0.2% strain offset, Ultimate Tensile Strength (UTS), % elongation, and % Reduction of Area for A709-PT from the three commercial heats against the ASME BPVC SA213/SA213M-23 [6] RT requirement. This comparison shows that A709-PT materials from all three heats satisfy the SA-213 RT requirement.

Table 3. RT tensile properties of A709-PT from the three commercial heats.

A709-PT Material	RT Tensile Test Number	YS, MPa	UTS, MPa	Elongation, %	Reduction of Area %
Commercial heat 1	1	359	747	40.0	52
	2	367	748	38.5	50.5
Commercial heat 2	1	328	701	43.3	48
	2	330	701	43.4	44.5
Commercial heat 3	1	305	694	44.0	46.5
	2	306	691	43.5	46.0
ASME SA-213 (minimum requirement)		270	640	30.0	Not required

The YS, UTS, % elongation, and % reduction of area from RT to 1000°C for A709-PT from the three commercial heats are shown in Figure 2. These tensile results show that their temperature dependence follows similar trends. The measured % elongation and % reduction of area show that the A709-PT materials from all three heats have good ductility from RT to 1000°C.

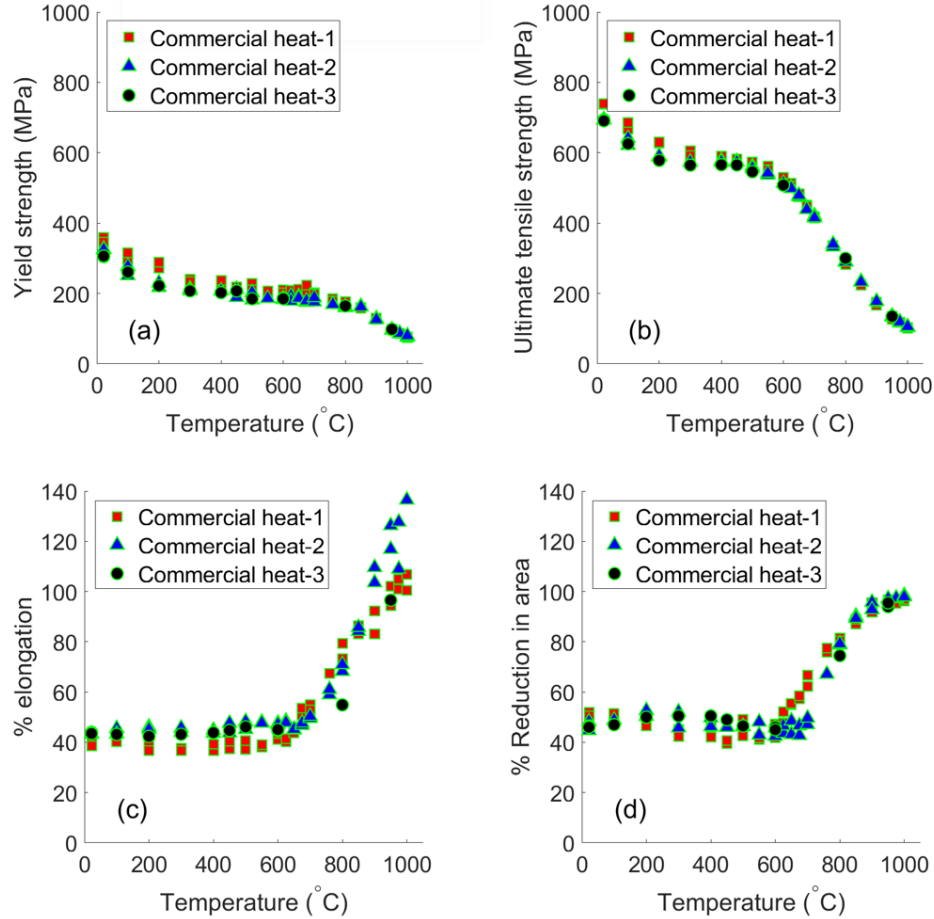


Figure 2. (a) Yield strength, (b) ultimate tensile strength, (c) % elongation, and (d) % reduction of area against temperature of A709-PT materials.

## 4. CREEP CODE CASE TESTING

A comprehensive creep test matrix for A709 was developed to support the development of ASME BPVC Section III, Division 5 code cases per the staged code qualification plan. Creep-rupture test data are being generated from the A709-PT materials from the three commercial heats. ANL, INL, and ORNL are each carrying out a subset of the creep code case testing matrix, and the testing sequence is arranged to best use the creep frames. All creep tests were conducted in accordance with ASTM E139-11 [9]. Figure 3 schematically shows the creep code case testing effort required in support of the staged code qualification plan. A series of code cases will be developed in progression under this stage code qualification plan, including the 100,000-hour code case (CC), 300,000-hour CC, and 500,000-hour CC.

Table 4 presents the FY 2023 creep-rupture testing status for the three commercial heats. The number of ruptured tests to date to support the respective code case and ongoing creep testing is summarized in this table. Note that these creep tests are planned and arranged to maximize utility of the creep machine and estimated test rupture time. All the planned long-term creep-rupture tests in support of 300,000-hour CC and 500,000-hour CC are ongoing on Heat 1 and Heat 2. The shorter-term creep-rupture testing in support of 100,000-hour CC has been completed on Heat 1 and has 37 ongoing creep tests on Heat 2 and 3.

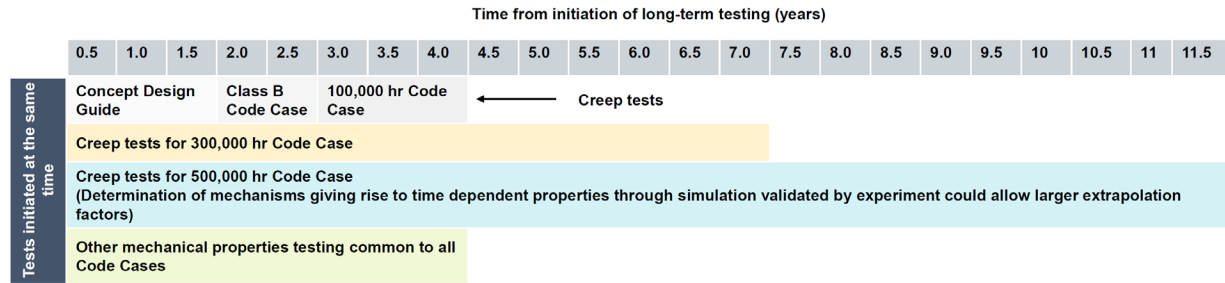


Figure 3. Creep code case testing in support of the staged code qualification plan.

Table 4. Summary of the creep code case testing on A709-PT from the three commercial heats.

Target Code Case	Number of Tests	
	Ruptured to date	Ongoing
100,000-hour CC	100	37
Long-term tests for 300,000-hour CC and 500,000-hour CC	—	12

The test matrix of ruptured and ongoing creep tests is presented in Figure 4. This figure has temperature in Celsius on the x-axis and stress in MPa on the y-axis. All ruptured tests on three different heats are shown with yellow square for Heat 1, red cross for Heat 2, and green triangle for Heat 3. All ongoing tests are shown in circle.

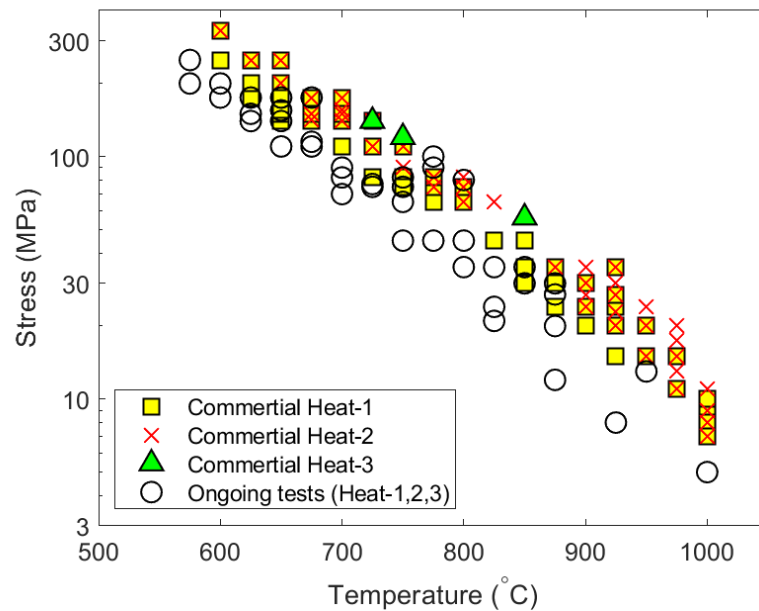


Figure 4. Finished and ongoing creep tests to support code case development on three commercial heats.

Figure 5 shows all creep-rupture data collected to date for the A709-PT materials from the three commercial heats. The x-axis is the test temperature, and the y-axis is the applied stress on the logarithmic (base 10) scale. The marker color represents the rupture life in hours as shown in a colormap

on the right side. This colormap is in the logarithmic scale covering creep-rupture life range of 100 hours to 20,000 hours.

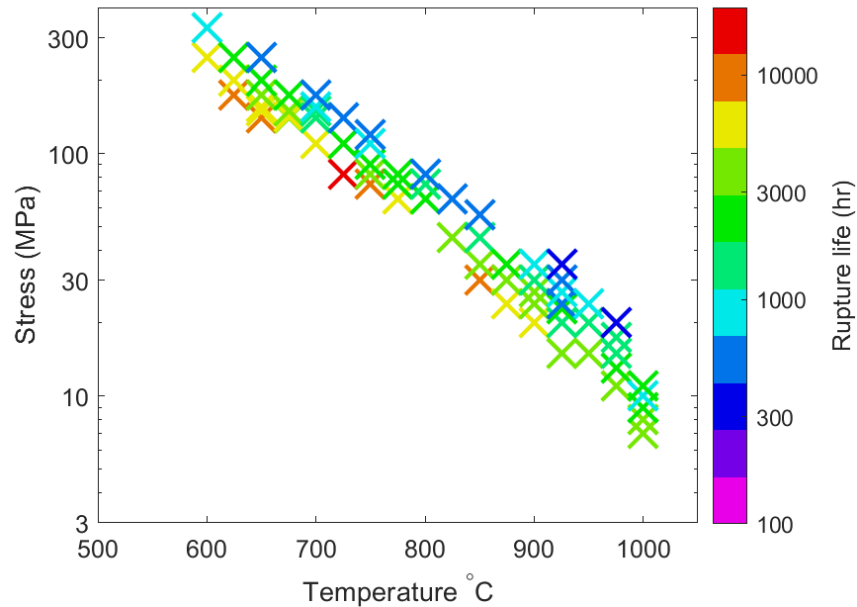


Figure 5. Creep-rupture data collected to date for the applied stresses and test temperatures shown. A709-PT materials from the three commercial heats.

## 5. FATIGUE AND CREEP-FATIGUE CODE CASE TESTING

A strain-controlled fatigue test matrix is planned to generate temperature-dependent fatigue design curves and creep-fatigue damage envelope as a key part of the A709 code case development at INL and ORNL. All fatigue tests presented in this report were conducted in accordance with ASTM E606/E606M-21 [10]. All test specimens were aligned with the rolling direction of the plate. Cylindrical test specimens were machined from the mid-thickness location of the plate for commercial Heat 1, and from the quarter thickness locations from the surfaces for Heats 2 and 3. Specimens tested at INL had minimum diameter of 7.49 mm, and specimens tested at ORNL had minimum diameter of 6.35 mm. INL used an extensometer with a gauge length of 12 mm, and ORNL used a 12.7-mm-long extensometer gauge. The test specimen geometries are shown in Figure 6 and Figure 7. All fatigue tests presented in this report were performed at 0.001/s strain rate and triangular strain waveform with fully reversed strain-controlled loading.



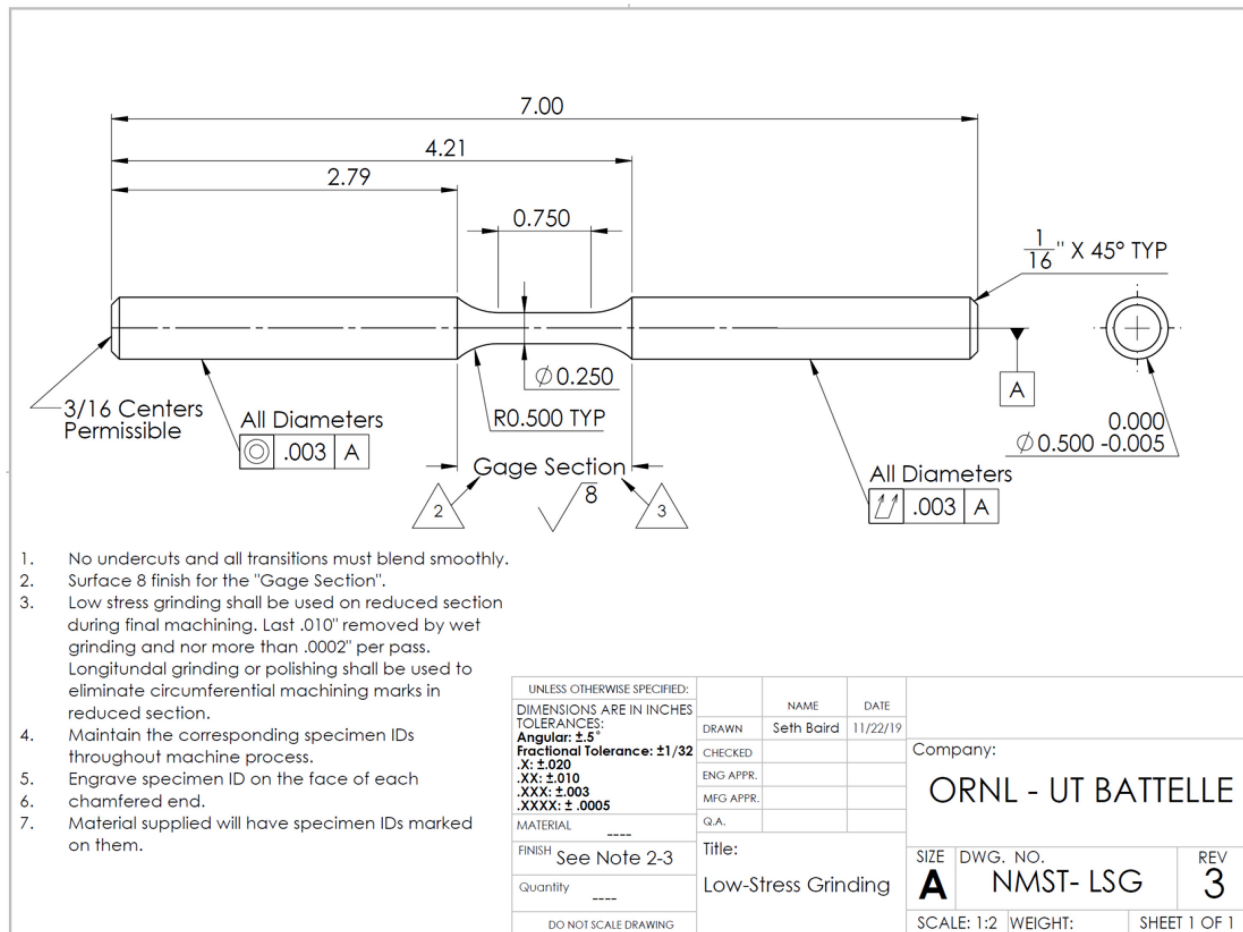


Figure 7. Test specimen geometry used at ORNL for fatigue and creep-fatigue tests. All dimensions are in inches.

The failure criterion is defined as the 20% drop in the ratio  $r$ , defined as the absolute ratio of the maximum stress to the minimum stress within a cycle, as was adopted in the Alloy 617 code case testing [11]. The schematic representation of the failure criteria is shown in Figure 8. The cycles to failure determined from the fatigue tests completed to date are plotted for various temperatures in Figure 9. These plots show the fatigue failure data of the A709-PT materials from Heat 1 and Heat 2, where the y-axis shows the strain range and the x-axis the cycles to failure per the 20% drop in  $r$  as the failure criterion. Fatigue testing of the A709-PT materials from the third heat has been initiated in FY 2023, and testing will continue next fiscal year.

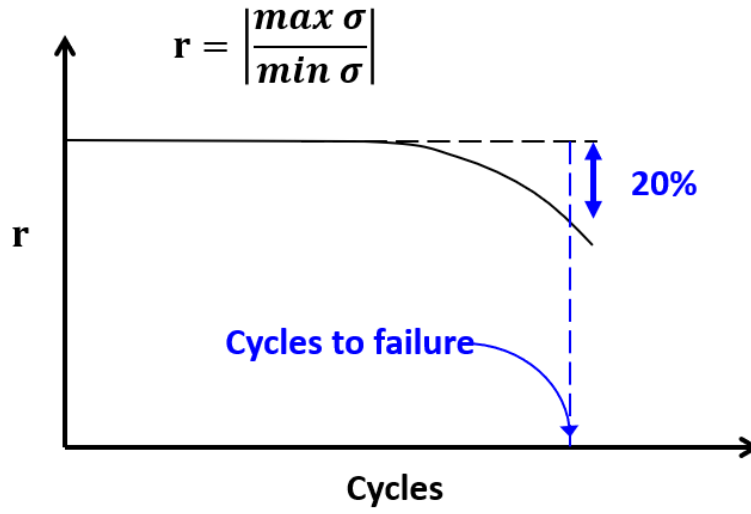


Figure 8. Schematic of the failure criterion to determine the cycles to failure in fatigue and creep-fatigue tests.

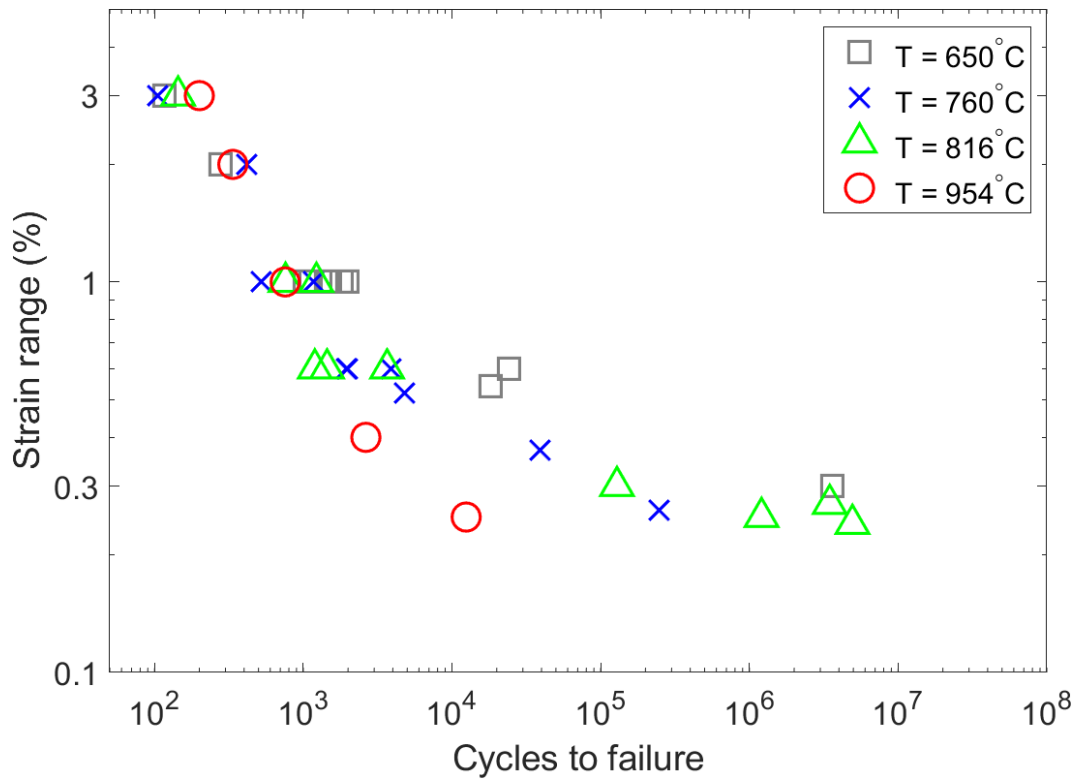


Figure 9. Number of cycles to failure against the applied strain range from the fatigue tests for the A709-PT materials from the first and second commercial heat for different temperatures.



In addition to obtaining the cycles to failure from a fatigue test, the stress values at peak-and-valley strains were collected for all the cycles. Furthermore, data for the stress and strain time histories for all the cycles were also collected. An example of a plot of the stresses at peak-and-valley strains as a function of cycles for different fatigue tests is presented in Figure 10. The y-axis is the stress in MPa and the x-axis is the number of cycles. The strain ranges for the fatigue tests are shown in the legend. The A709-PT materials were from the second heat and the test temperature was 954°C.

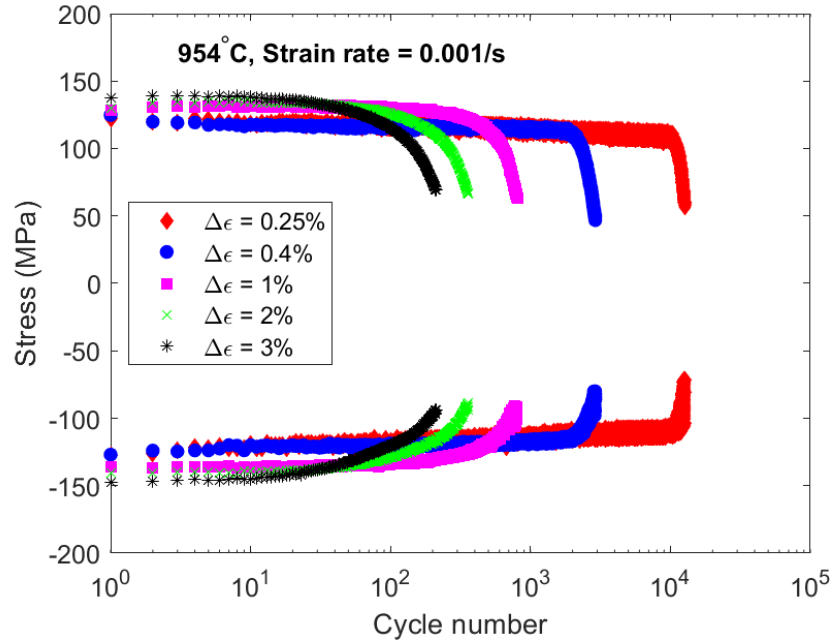


Figure 10. Comparison of the peak-and-valley stress plots for fatigue tests at 954°C with different strain ranges.

A schematic figure of the strain-controlled creep-fatigue load cycle is shown in Figure 11. The tensile strain was applied to specimen and held constant for desired hold time followed by complete strain reversal. Creep-fatigue code case testing for the A709-PT materials from Heat 1 and Heat 2 made significant progress with tests at different temperatures, strain ranges, and hold times. The testing on the A709-PT materials from Heat 3 was initiated in FY 2023 and will continue next FY. All creep-fatigue tests were performed in accordance with the ASTM E2714-13 [12].

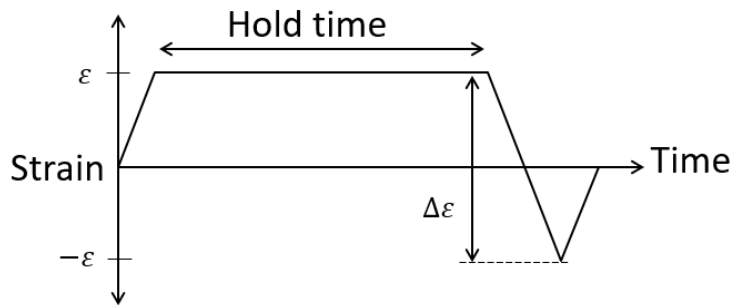


Figure 11. Schematic figure showing a typical strain-controlled creep-fatigue load cycle.

The creep-fatigue test data was analyzed by calculating the creep and fatigue damage fractions separately. The fatigue damage fraction ( $D_f$ ) is the ratio of the cycles to failure ( $N$ ) in a creep-fatigue test to the cycles to failure ( $N_{rf}$ ) in a separate fatigue test for the same strain range, but at a rapid enough strain rate where creep damage effect would be small. The ( $D_f$ ) calculation is shown in Equation 1. The creep damage fraction ( $D_c$ ) is the summation of creep damage accumulated within each cycle ( $dD_{c,i}$ ) as shown in Equation 2. The creep damage accumulated within a given cycle is calculated by using the time fraction approach. In this approach, the stress relaxation history during the strain hold is used to determine the time history of time-to-rupture ( $T_D$ ) from the Larson-Miller correlation. Then integration over the hold time is performed per Equation 3 to determine ( $dD_{c,i}$ ).

$$D_f = \frac{N}{N_{rf}} \quad (1)$$

$$D_c = \sum_{i=1}^n dD_{c,i} \quad (2)$$

$$dD_{c,i} = \int_{t_{0,i}}^{t_{h,i}} \frac{1}{T_D} dt \quad (3)$$

The calculated creep-fatigue damages from different tests for the A709-PT materials from all three heats are presented in the creep-fatigue interaction plot of Figure 12 shown in logarithmic (base 10) scales. The bilinear interaction envelopes with three different sets of intersection points (0.1-0.1, 0.2-0.2, and 0.3-0.3) in dashed lines are compared against the creep-fatigue test results. These interaction lines are not the lower bound curves, but they provide some possible creep-fatigue damage envelopes for design evaluations.

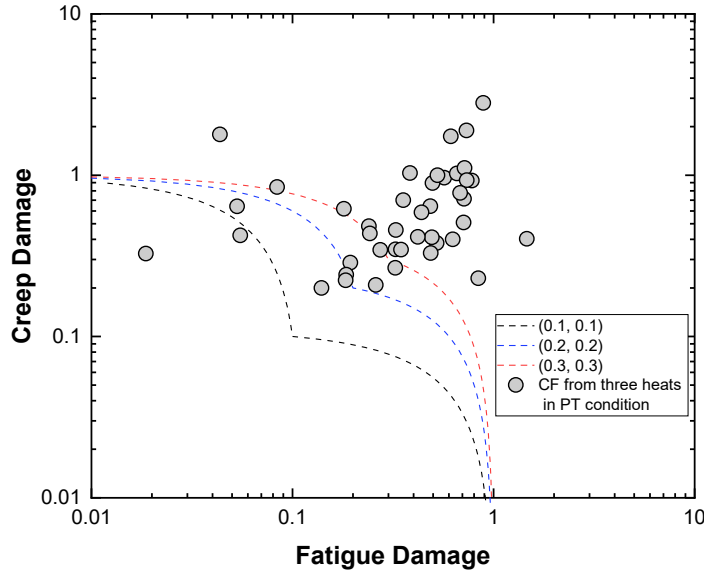


Figure 12. Creep-fatigue data plotted in the form of a creep-fatigue interaction diagram for A709-PT materials from three commercial heats.

## 6. WELDS AND WELDMENT DEVELOPMENT

As part of the A709 code qualification effort, ORNL has been conducting research to develop the technical basis for A709 weld fabrication and qualification. So far, the research has been focused on using A709 weld wires as the matching filler metal to weld A709 plates. The matching filler metal is expected to provide the best corrosion and mechanical performance, compared to the use of filler metals with different chemistries, although the later may offer improved weldability.

An initial scoping study on experimental heats of A709 plates revealed potential issues of weld solidification cracking when the level of impurities such as phosphorous is high but still within the specification in ASME BPVC Section II A213/A213M-23 [6]. Only the weldment with very low phosphorous content of less than 0.002 wt.% (20 parts per million by weight, wppm) in both the base metal plate and the matching filler metal passed the ASME BPVC Section IX [13] weldment qualification tests.

Computational non-equilibrium solidification calculations found that phosphorous has the most important impact on expanding the solidification temperature, which is detrimental to the solidification process as it would subject the mushy zone (liquid-solid co-exist region) to high-tensile stress due to the thermal contraction of the weld on cooling and causes solidification cracking. Increasing the levels of phosphorous from 0.002 wt.% (20 wppm) to 0.018 wt. % (180 wppm) led to the increase of solidification temperature range over 300°C [14]. The modeling results set the foundation for a strategic plan to solve the solidification cracking issue and to weld A709 materials having a wider range of chemistries. One strategy would be to limit the phosphorous level of the weld wire when welding A709 base metal having relatively high phosphorous.

### 6.1 Fabrication and Qualification Testing of A709 Production Welds

Following the strategy of limiting the phosphorous level of the A709 weld wire, two A709 production welds, designated W10 and W11, were fabricated. The A709-PT materials from the first two commercial heats were used the base metal, and the welding procedure was the one developed on the test welds in FY 2022 [15, 16]. The two commercial heats base metal plates had phosphorous level of 140 wppm and 30 wppm, respectively. The A709 filler metal had phosphorous content less than 20 wppm [16]. The welding process was gas tungsten arc welding (GTAW). Details of these two production welds are listed in Table 5, and photographs of the two welds are shown in Figure 13. Both production welds passed ASME BPVC Sec. IX weld qualification tests on X-ray inspection, side-bend testing and RT tensile.

Further comprehensive microstructure characterization showed no detectable welding defects on these two production welds [16]. It is noted that the commercial Heat 1 A709 plates have relatively high-phosphorous level of 140 wppm, and the commercial Heat 2 plates are 2 inches thick. Thus, the A709 welding procedure development enabled the fabrication of a wide range of A709 welds using industrial standard GTAW process.

Table 5. A709 production welds.

A709 Welds		Production Weld – W10	Production Weld – W11
Alloy 70 filler metal weld Wire	Phosphorous Level (wppm)	<20	<20
	Heat No. of the supply material for weld wire	011367-08	011367-08
	Wire dia. (in)	0.035	0.035
A709-PT base metal plates	Heat No.	Commercial Heat 1, Heat 58776	Commercial Heat 2, Heat 529900

A709 Welds		Production Weld – W10	Production Weld – W11
	Thickness (in)	1.12	2.05
	Phosphorous Level (wppm)	140	30
Total weld length (in)		15	27.5
Weld joint geometry		20-degree single V	20-degree double V
ASME Sec. IX Weld Qualification	X-Ray	Pass	Pass
	Side Bend	Pass	Pass
	RT Tensile	Pass	Pass



(a)



(b)

Figure 13. Photographs of the A709 production welds: (a) W10 and (b) W11.

Additional research on A709 welding at ORNL has been performed to relax the restriction of the phosphorous content in the A709 filler metal weld wire, with the objective to determine a practical upper limit of phosphorous level without solidification cracking. To this end, welding procedures such as heat input level, welding sequences were further systematically investigated and improved. A series of ASME BPVC Section IX qualified welds were fabricated using weld wires with increasing levels of phosphorous content. The base metal used for these studies was the A709-PT materials from the first commercial heat (Heat 58776) with a high-phosphorous level of 140 wppm [15–18]. In FY 2023, ORNL has demonstrated that it is possible to successfully weld with 80-wppm phosphorous weld wire, on the A709-PT materials from the commercial heat having 140-wppm phosphorous. The weld successfully passed all the ASME BPVC Section IX code qualification tests [18].

This study concludes that A709 matching filler metal with moderate level of phosphorous (<80 wppm) could be acceptable to produce code qualified A709-PT welds with the GTAW process widely used in the nuclear industry. Nevertheless, the best practice of welding would always keep the phosphorous level in the weld wire as low as possible to minimize concerns of weld solidification cracking.

## 6.2 Code Case Testing of A709 Welds

As part of the code qualification data package in developing the stress reduction factors of A709 welds, cross-weld creep-rupture code case testing is being completed at ORNL on the test welds and the two production welds. The preliminary cross-weld creep tests results continue to show little or no creep strength reduction relative to the base metal [16,18]. Creep-rupture testing on A709 cross-welds continued in FY 2023, and data are being generated to support the submittal of the first A709 Code Case to ASME by 2025.

## 7. SUMMARY

This report summarizes the status of the tensile, creep, fatigue, and creep-fatigue testing to date conducted at ANL, INL and ORNL on precipitation treated A709 from three commercial heats. The developed test data are used to update the data package required to qualify A709 in ASME BPVC Section III, Division 5. The Section III, Division 5 A709 code case for Class A construction requires the data collected from at least three commercial heats. An extensive set of test data generated for the A709-PT materials from two commercial heats and some initial test results from the third commercial heat has been collected and presented in this report. The RT tensile properties for A709-PT materials from all three heats met the specification minimum of the ASME BPVC Section II Part A SA-213/SA-213M specification for Grade TP310MoCbN (UNS S31025) requirement for seamless tubing. The fatigue and creep-fatigue test results completed to date for the A709-PT materials from two commercial heats are presented.

## 8. REFERENCE

- [1] ASME (2023) “BPVC Section III Rules for Construction of Nuclear Facility Components-Division 5-High Temperature Reactors.” American Society of Mechanical Engineers. BPVC-III.5 – 2023.
- [2] T.-L. Sham and K. Natesan, “IAEA-CN245-074 Code Qualification Plan for an Advanced Austenitic Stainless Steel, Alloy 709, for Sodium Fast Reactor Structural Applications IAEA-CN245-074,” in *International Conference on Fast Reactors and Related Fuel Cycles: Next Generation Nuclear for Sustainable Development (FR17)*. 2018, no. June 2017, pp. 1–10, [Online]. Available: <http://energy.gov/downloads/doe-public-access-plan>.
- [3] Michael D. McMurtrey, and Ryann E. Rupp. (2019) *Report on FY19 scoping creep and creep-fatigue testing on heat treated Alloy 709 base metal*. INL/EXT-19-55502-Rev000. Idaho National Laboratory, Idaho Falls, Idaho.
- [4] X. Zhang, T. L. Sham, and G. A. Young. (2019) *Microstructural Characterization of Alloy 709 Plate Materials with Additional Heat Treatment Protocol*. ANL-ART-170. Argonne National Laboratory, Argonne, Illinois.
- [5] Sham, Ting-Leung, Ryann Elizabeth Bass, Yanli Wang, and Xuan Zhang. (2022) *A709 Qualification Plan Update and Mechanical Properties Data Assessment*. INL/RPT-22-67641-Rev000. Idaho National Laboratory, Idaho Falls, Idaho. United States.
- [6] ASTM International (2023) “Standard Specification for Seamless Ferritic and Austenitic Alloy-Steel Boiler, Superheater, and Heat-Exchanger Tubes.” ASTM A213/A213M-23.
- [7] ASTM International. (2021) “Standard Test Methods for Tension Testing of Metallic Materials.” ASTM E8/E8M-21.

- [8] ASTM International (2021) “Standard Test Methods for Elevated Temperature Tension Tests of Metallic Materials.” ASTM E21-20.
- [9] ASTM International (2018) “Standard Test Methods for Conducting Creep, Creep-Rupture, and Stress-Rupture Tests of Metallic Materials.” ASTM E139-11.
- [10] ASTM International (2021) “Standard Test Method for Strain-Controlled Fatigue Testing.” ASTM E606/E606M-21.
- [11] Richard Wright (2021) *Draft ASME Boiler and Pressure Vessel Code Cases and Technical Bases for Use of Alloy 617 for Constructions of Nuclear Component Under Section III, Division 5*. INL/EXT-15-36305, Revision 2. Idaho National Laboratory, Idaho Falls, Idaho.
- [12] ASTM International (2020) “Standard Test Method for Creep-Fatigue Testing.” ASTM E2714-13.
- [13] ASME (2023) “BPVC Section IX Welding, Brazing and Fusing Operators-Qualification Standard for Welding, Brazing, And Fuzing Procedures; Welders; Brazers; And Welding, Brazing, And Fusing Operators.” American Society of Mechanical Engineers. BPVC-IX – 2023.
- [14] Z. Feng, J. M. Vitek, T. Liu, and Y. Wang (2018) *Evaluation of the Effect of Alloy Chemistry on the Susceptibility of Weld Solidification Cracking of Alloy 709 Weldment and Development of Mitigation Strategy*. ORNL/TM-2018/965. Oak Ridge National Laboratory, Oak Ridge, Tennessee.
- [15] Z. Feng, T. Dai, D. Kyle, Wang, and Y. Wang (2020) *Welding Parameters Optimization and the Fabrication of Qualified Alloy 709 Welds*. ORNL/TM-2020/1706. Oak Ridge National Laboratory, Oak Ridge, Tennessee.
- [16] Z. Feng, T. Dai, D. Kyle, Y. Wang, and Y. Wang (2021) *Report on FY 2021 Fabrication and Testing of Qualified Alloy 709 Welds at ORNL*. ORNL/TM-2021/2171. Oak Ridge National Laboratory, Oak Ridge, Tennessee.
- [17] Z. Feng, Y. Wang, D. Kyle, and T. Dai (2019) *Report on FY19 Fabrication and Evaluation of Weldment for Alloy 709 Commercial Heat Plates*. ORNL/TM-2019/1320. Oak Ridge National Laboratory, Oak Ridge, Tennessee.
- [18] Z. Feng, Y. Wang, J. Ward, and Y. Wang (2023) *Report on FY 2023 Welding R&D at ORNL in Support of ASME Alloy 709 Code Case Development*. ORNL/TM-2023/3045. Oak Ridge National Laboratory, Oak Ridge, Tennessee.